P H Y S I C A L  R E V I E W  L E T T E R S

# Wetting, Drying, and Layering of Colloid-Polymer Mixtures at Porous Interfaces

Paul P. F. Wessels,[1] Matthias Schmidt,[2,*] and Hartmut Löwen[1]

[1]*Institut für Theoretische Physik II, Heinrich-Heine-Universität Düsseldorf, Universitätsstraße 1, 40225 Düsseldorf, Germany*
[2]*Soft Condensed Matter Group, Debye Institute, Utrecht University, Princetonplein 5, 3584 CC Utrecht, The Netherlands*
(Received 25 September 2004; published 24 February 2005)

The influence of interface porosity on the wetting properties of colloid-polymer mixtures is studied within density functional theory for the Asakura-Oosawa-Vrij model at the surface of a quenched hard-sphere matrix. While the porosity hardly changes the location of the transition from partial to complete wetting at colloidal bulk gas-liquid coexistence, the onset of wetting, as signaled by the first discontinuous layering transition, can be efficiently controlled by tailoring the porosity. We furthermore find that the penetrability of the porous interface induces complete drying into the matrix upon approaching capillary coexistence.

Close to gas-liquid coexistence, the liquid phase can wet a substrate although the gas is stable in bulk. Research in the last decades [1,2] has revealed that the wetting behavior depends crucially on the microstructure of the substrate. This knowledge has led to various applications like, e.g., exploiting the lotus effect to arrive at self-cleaning surfaces [3]. In particular, various phenomena like imbibition, sorption, and liquid infiltration, relevant for inking and printing techniques, are initiated by wetting on a *porous* interface. In order to achieve a fundamental understanding, the spreading kinetics of different liquid droplets on porous substrates has been investigated using polymer solutions [4] and oil droplets [5]. A proper theoretical description of wetting on porous interfaces based on the molecular interactions, however, is still in its infancy. This situation is in contrast to the cases of rough [6], chemically [1,7,8], or topographically [9,10] structured substrates. Interface porosity is expected to alter the wetting characteristics due to permeation of the liquid into the substrate. Moreover, different wetting scenarios can occur at the inner interface of the porous material and on top of a porous surface, since due to capillary condensation deep inside the porous material, the gas-liquid coexistence line is displaced in the phase diagram relative to that of the free bulk system.

Colloidal dispersions are excellent model systems to study interfacial phenomena. The addition of nonadsorbing polymers to dispersions of colloidal particles generates an effective attraction between the colloids due to the depletion effect. The strength and range of the attraction can be controlled through the polymer concentration and size, respectively [11]. Under appropriate conditions macroscopic phase separation occurs into colloid-rich (liquid-like) and colloid-poor (gaslike) phases [12]. Such colloid-polymer mixtures allow the study of fundamental interfacial phenomena using real space techniques (see, e.g., [13]). Wetting of various substrates has been investigated experimentally [14,15], and there is the fascinating possibility to prepare well-defined model porous media composed of aggregated colloidal rods or spheres [16]; the

latter realize a model used frequently in theory (see, e.g., [17,18]).

In this Letter, we study the influence of interface porosity on the wetting behavior of colloid-polymer mixtures. We use the standard Asakura-Oosawa-Vrij (AOV) model of sterically stabilized (hard-sphere) colloids mixed with nonadsorbing ideal polymers and expose it to the planar surface of a model porous matrix composed of quenched (immobilized) hard spheres. We calculate the induced wetting behavior using a recent density functional theory [19,20] that has been shown to reliably describe details of wetting and layering for hard structureless walls [21,22]. We systematically study the location of the complete wetting point of the porous interface and that of the first layering transition indicating the onset of wetting. We find that interface porosity drastically affects the location of the first layering transition but hardly influences the location of the wetting transition. In particular, matrices with porosities compatible with the colloid size strongly favor the onset of wetting. This finding can be exploited to tailor substrates with optimal wetting properties leading to potential applications for microfluidic devices. Furthermore, we find complete drying at the inner porous interface and as well as wetting on top of the interface depending on the statepoint. This is a scenario involving *two* different interfacial phenomena. As a consequence, a liquid-filled porous material will dry from its free boundaries upon approaching capillary gas-liquid coexistence [23]. All our predictions can in principle be assessed in experimental colloid-polymer mixtures exposed to porous substrates.

Our model consists of the AOV description [11] of hard-sphere colloids (species $c$) and ideal polymer spheres (species $p$), brought into contact with a porous matrix of quenched immobilized hard spheres (species $m$), see Fig. 1. The pair interaction potential between particles of species $ij \neq pp$ is that of hard spheres: $\phi_{ij}(r) = \infty$ if $r < (\sigma_i + \sigma_j)/2$ and zero otherwise, where $\sigma_i$ is the diameter of particles of species $i = c, p, m$, and $r$ is the center-to-center distance. The pair interaction between polymers
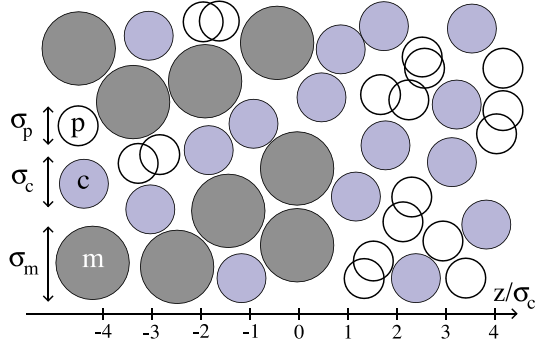
FIG. 1 (color online).   Illustration of the model of hard-sphere colloids (light blue) and ideal polymer coils (white) adsorbed against the porous surface of a matrix of quenched hard spheres (dark gray). The matrix particles are distributed homogeneously in the half-space $z < 0$; only colloids and polymers are mobile.

vanishes for all distances: $\phi_{pp}(r) = 0$. This system is characterized by the size ratios between polymers and colloids, $q = \sigma_p/\sigma_c$, and between matrix particles and colloids, $\sigma_m/\sigma_c$. Packing fractions are denoted by $\eta_i = V_i\rho_i$, where $\rho_i$ is the number density and $V_i = \pi\sigma_i^3/6$ is the particle volume of species $i = c, p, m$. The chemical potentials of species $i = c, p$ are denoted by $\mu_i$, and we also use the packing fraction in a polymer reservoir in equilibrium with the system, $\eta_{p,r} = V_p \exp(\beta\mu_p)$, where $\beta = 1/(k_B T)$, $k_B$ is the Boltzmann constant and $T$ is temperature. To model the matrix surface we cut away a half-space from a homogeneous matrix [distributed according to the hard core interaction $\phi_{mm}(r)$ in the absence of colloids and polymers]. The resulting density distribution for the centers of the matrix spheres is $\rho_m(z) = \eta_m/V_m$ for $z < 0$ and zero otherwise, where $z$ is the coordinate perpendicular to the surface.

We use a recently developed fundamental measure density functional theory for this quenched-annealed mixture [19,20]. Equilibrium distributions are obtained from the grand potential functional, $\Omega[\rho_c(\mathbf{r}), \rho_p(\mathbf{r}); \rho_m(\mathbf{r})]$, by numerical minimization, $\delta\Omega/\delta\rho_c(\mathbf{r}) = 0$ and $\delta\Omega/\delta\rho_p(\mathbf{r}) = 0$, where $\rho_m(\mathbf{r})$ serves as a fixed input field. The required "double average" over colloid-polymer configurations and over matrix realizations is taken into account properly in this framework; rather treating the matrix particles via an explicit external potential would be tedious, if not prohibitive. A key quantity measuring the change of particle number due to the presence of the interface is the (excess) adsorption $\Gamma_i$ of species $i = c, p$ as obtained from $\Gamma_i = \int_{-\infty}^{0} dz[\rho_i(z) - \rho_i(-\infty)] + \int_0^\infty dz[\rho_i(z) - \rho_i(\infty)]$, such that the Gibbs dividing surface is located at $z = 0$. Possible measurements of $\Gamma_i$ involve the need to determine the average densities inside the porous matrix, $\rho_i(-\infty)$; we imagine that using real space techniques like confocal microscopy [13,14] in conjunction with transparent (not fluorescently labeled) matrix particles can facilitate this task. The interface tension, $\gamma$, is obtained from the differ-

ence of grand potentials in the inhomogeneous situation and that of two bulk half-spaces, $\gamma = (\Omega[\rho_c(z), \rho_p(z); \rho_m(z)] - \Omega_+ - \Omega_-)/A$, where $\Omega_\pm$ is the grand potential of a homogeneous half-space with constant densities $\rho_c(\pm\infty)$, $\rho_p(\pm\infty)$, $\rho_m(\pm\infty)$, and $A$ is the area of the interface. In the following, we restrict ourselves to the size ratio $q = 0.6$, large enough to induce stable fluid-fluid demixing.

We first consider a matrix with high packing fraction, $\eta_m = 0.5$, such that the (capillary) phase behavior inside the matrix plays a minor role as adsorption in the bulk matrix is strongly suppressed. Figure 2(a) shows the phase diagram of the AOV model as a function of $\eta_{p,r}$ and $\eta_c$, the latter being the colloid packing fraction in the free bulk, $z \to \infty$. The density functional theory result for the bulk binodal is equivalent to that from free-volume theory [12]. The mixture in contact with the porous interface exhibits purely entropy-driven surface phases. On the gas side of the bulk gas-liquid binodal, at high values of $\eta_{p,r}$ ($\gtrsim 1$), the colloid density profile is practically gaslike and shows only a tiny amount of colloid adsorption at the interface. Upon reducing $\eta_{p,r}$, there occurs a discontinuous surface phase transition from this gaslike state to a state with one adsorbed colloid layer. This transition possesses an accompanying adsorption spinodal point at still lower values of $\eta_{p,r}$, where the gaslike state loses its metastability. The first layering transition can be viewed as a precursor of the wetting transition, which occurs upon reducing $\eta_{p,r}$ further. Such a pattern of phase transitions has been found previously for the AOV model exposed to a hard *smooth*
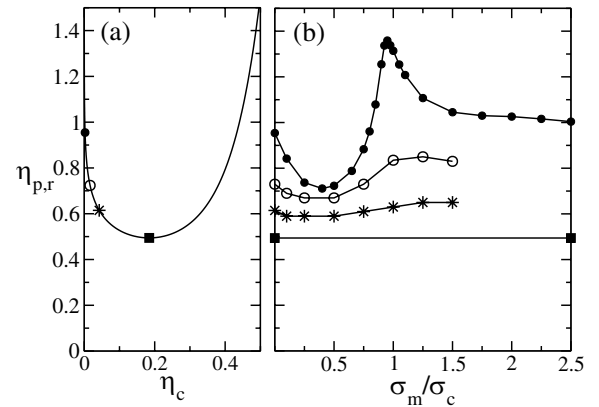


FIG. 2.   Interfacial phase behavior of the model colloid-polymer mixture of size ratio $q = 0.6$ adsorbed against the surface of a porous matrix with varying interface porosity. (a) Phase diagram as a function of $\eta_c$ and $\eta_{p,r}$. Shown are characteristic points on the free bulk gas-liquid binodal (full curve): first layering transition (filled circle), accompanying adsorption spinodal point (open circle), wetting transition (star) at a smooth planar hard wall, and bulk critical point (filled square). (b) Location, in $\eta_{p,r}$, of these characteristic points [same symbols as in (a)] vs size ratio $\sigma_m/\sigma_c$ for $\eta_m = 0.5$. The smooth planar hard wall results shown in (a) are recovered for $\sigma_m/\sigma_c \to 0$.

wall [21,24], and indeed we recover these earlier findings in the limit of vanishing matrix particle size, $\sigma_m/\sigma_c \to 0$ and $\eta_m = \text{const}$, and hence $\rho_m \to \infty$.

Strikingly, the location of these surface phase transitions depends strongly on the relative size of the matrix particles, $\sigma_m/\sigma_c$. Increasing $\sigma_m/\sigma_c$ from 0, the location of the first layering transition moves to smaller values of $\eta_{p,r}$, reaches a minimum at around $\sigma_m/\sigma_c = 0.4$, and then increases dramatically (by about a factor of 2) until $\sigma_m/\sigma_c = 0.95$. Further increasing $\sigma_m/\sigma_c$ beyond 0.95, the value of $\eta_{p,r}$ at the layering transition decreases again smoothly. The accompanying jump in colloid adsorption remains of the order of $3.6/\sigma_c^2$ in the regime $\sigma_m/\sigma_c = 1.5 - 2.5$, so the transition seems to persist without indication of a terminal critical point. In contrast, the adsorption spinodal point and the location of the wetting transition are affected only little by variation of $\sigma_m/\sigma_c$. Both also pass through a minimum around $\sigma_m/\sigma_c \approx 0.4$, though much less pronounced, and lack any strong peak. In order to illustrate the structure associated with the surface phase behavior, we plot colloid density profiles for four representative size ratios in Fig. 3. As the first layering transition is at the bulk binodal, both the gaslike state and the state with one adsorbed colloid layer are in coexistence with the liquid state against the wall. Increasing $\sigma_m/\sigma_c$, the interface becomes increasingly penetrable and the colloid density profile becomes smoother and less modulated. We have calculated contact angles using Young's equation, $\cos\theta = (\gamma_{wg} - \gamma_{wl})/\gamma_{lg}$, with $\gamma_{wg}$, $\gamma_{wl}$, and $\gamma_{lg}$ being the wall-gas, wall-liquid, and gas-liquid [24] interfacial tensions at bulk coexistence, respectively. We obtain the sequence $\theta = 18.2°, 8.1°, 7.7°, 3.6°$ for the statepoints shown in Figs. 3(a)–3(d), respectively [25]. All these findings are consistent with the observation that for $\sigma_m/\sigma_c = 1$, the matrix is in effect

a quenched liquid that stabilizes colloid adsorption at the interface. For increasing $\sigma_m/\sigma_c > 1$ the matrix becomes increasingly penetrable and the significant amounts of capillary condensed liquid inside the matrix again stabilizes adsorption of colloidal liquid.

For moderate matrix packing fractions, adsorption in the bulk matrix is relevant, and we have chosen $\eta_m = 0.2$ and $\sigma_m/\sigma_c = 1$ for a detailed study of the surface phase behavior. The bulk phase diagram, displayed in Fig. 4(a), possesses two gas-liquid binodals, that in the free bulk and that deep inside the matrix. Considering the colloidal gas at coexistence in the bulk outside the matrix against the porous interface, we have again located the first layering transition, the layering spinodal point and the wetting transition. Moreover, we find complete drying of the interface for all $\eta_{p,r}$ (we have gone as high as $\eta_{p,r} = 2$) upon approaching capillary coexistence from the liquid side in the phase diagram. This provides a clear mechanism for desorption. To illustrate the behavior, we monitor the colloid adsorption at the interface, $\Gamma_c$, along three different paths at constant values of $\eta_{p,r}$ through the phase diagram, see Fig. 4(b). For $\eta_{p,r} = 0.55$, $\Gamma_c$ diverges upon approaching the binodal of the free bulk, as expected in the complete wetting regime. For $\eta_{p,r} = 1$, the path crosses both bi-
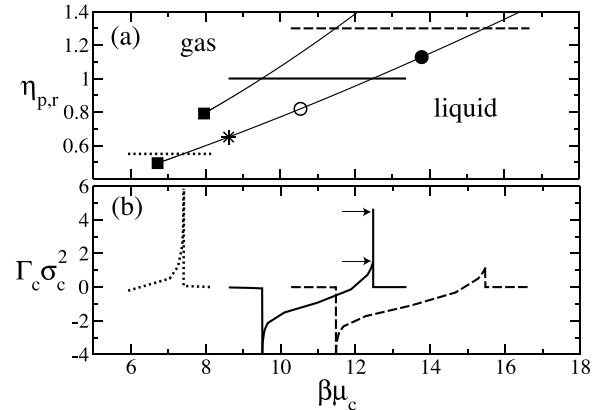


FIG. 4. Interfacial properties of the model colloid-polymer mixture at the surface of a porous matrix for $q = 0.6$, $\sigma_m/\sigma_c = 1$, and $\eta_m = 0.2$. (a) Phase diagram as a function of colloid chemical potential, $\beta\mu_c$, and polymer reservoir packing fraction, $\eta_{p,r}$. Shown is the gas-liquid binodal in the free bulk (lower thin line) and inside the matrix (upper thin line), either one ending in a critical point (filled square). On the gas side of the free bulk binodal there occurs the first layering transition (filled circle), the layering spinodal point (open circle), and the wetting transition (star). Shown are representative paths at constant polymer fugacities of $\eta_{p,r} = 0.55$ (dotted line), 1 (thick line), and 1.3 (dashed line). (b) The colloid adsorption, $\Gamma_c\sigma_c^2$, as a function of $\beta\mu_c$ corresponding to the paths in (a), and displaying complete wetting (dotted line), complete drying and the layering transition (thick line, arrows indicate the jump in $\Gamma_c$ at the transition), and complete drying and partial wetting (dashed line).
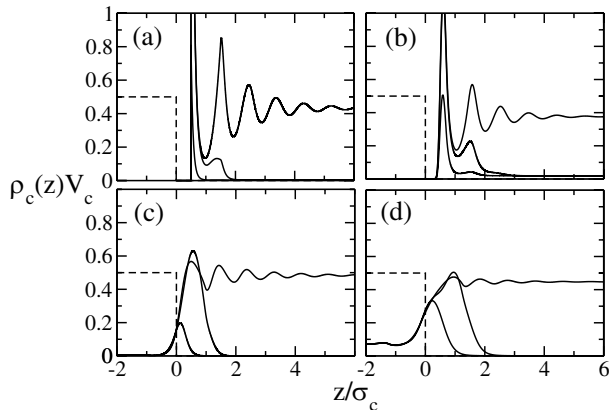


FIG. 3. Density profiles at the layering transition for $q = 0.6$ and $\eta_m = 0.5$ corresponding to Fig. 2. Shown are results for the coexisting gaslike state, the surface state with one adsorbed colloid layer, and the coexisting liquid state (full lines, from bottom to top), as well as the matrix density profiles (dashed lines, $\rho_m(z)V_m$) for $\sigma_m/\sigma_c = 0$ (a), 0.4 (b), 0.95 (c), and 1.5 (d). Polymer density profiles are omitted for clarity.

nodals with diverging (negative) adsorption at the matrix binodal, indicating complete drying, and finite adsorption at the free bulk binodal, indicating partial wetting. On approaching the free bulk binodal from the gas side, there is a jump in $\Gamma_c$ just before coexistence, indicating the crossing of the first layering line off-bulk coexistence. For $\eta_{p,r} = 1.3$ again complete drying on the (liquid side of the) capillary binodal and partial wetting at the free bulk binodal is found, but without crossing a layering transition. For the cases of diverging adsorption we have checked that $\Gamma_c \sim \ln|1 - \mu_c/\mu_c^{coex}|$, with $\mu_c^{coex}$ the chemical potential at coexistence, over more than two decades of $|1 - \mu_c/\mu_c^{coex}|$. Finally, essentially vanishing excess adsorption is found on approaching the capillary binodal from the gas side and the free bulk binodal from the liquid side.

In conclusion, we have investigated interfacial effects at an external surface of a random porous medium using colloid-polymer mixtures as a model adsorbate. The location of the layering surface phase transition from a gaslike state to a state with one clear adsorbed colloid layer depends strikingly on the porosity, as measured by the size ratio of mobile and quenched colloids, while the location of the transition from partial to complete wetting shows similar, albeit quantitatively weaker dependence. Both the order of the wetting transition and the existence of further layering transitions, as appear in the case of the smooth planar wall [24], are more subtle. The liquid phase condensed inside the matrix dries completely from the matrix surface as the capillary binodal is approached from the liquid side. In contrast, the gas phase inside the matrix is not macroscopically affected by approaching the capillary binodal from the gas side. This possibly provides an alternative mechanism, in equilibrium, for Rosinberg *et al.*'s observation [23], that introducing an external interface may have a major influence on the hysteresis in sorption curves. In experimental realizations of our model, porous interfaces are readily constructed by sedimenting heavy colloids or using laser tweezers [26]. In combination with suitable colloid-polymer mixtures (density- and indexed-matched in order to circumvent sedimentation and laser trapping, respectively), interfacial behavior corresponding to that investigated here could be studied [14,15]. In addition, such systems can be tackled with computer simulations to test our predictions.

*Present address: Institut für Theoretische Physik II, Heinrich-Heine-Universität Düsseldorf, Universitätsstraße 1, 40225 Düsseldorf, Germany

[1] R. Lipowsky, Curr. Opin. Colloid Interface Sci. **6**, 40 (2001).

[2] H. Gau, S. Herminghaus, P. Lenz, and R. Lipowsky, Science **283**, 46 (1999).

[3] C. Neinhuis and W. Barthlott, Annals of Botany (London) **79**, 667 (1997).

[4] R. K. Holman, M. J. Cima, S. A. Uhland, and E. Sachs, J. Colloid Interface Sci. **249**, 432 (2002).

[5] V. M. Starov, S. A. Zhdanov, S. R. Kosvintsev, V. D. Sobolev, and M. G. Velarde, Adv. Colloid Interface Sci. **104**, 123 (2003).

[6] M. Kardar and J. O. Indekeu, Europhys. Lett. **12**, 161 (1990).

[7] C. Bauer and S. Dietrich, Phys. Rev. E **61**, 1664 (2000).

[8] P. Lenz, C. Bechinger, C. Schäfle, P. Leiderer, and R. Lipowsky, Langmuir **17**, 7814 (2001).

[9] M. Heni and H. Löwen, Phys. Rev. Lett. **85**, 3668 (2000).

[10] C. Rascon and A. O. Parry, Nature (London) **407**, 986 (2000).

[11] S. Asakura and F. Oosawa, J. Chem. Phys. **22**, 1255 (1954); A. Vrij, Pure Appl. Chem. **48**, 471 (1976).

[12] H. N. W. Lekkerkerker, W. C. K. Poon, P. N. Pusey, A. Stroobants, and P. B. Warren, Europhys. Lett. **20**, 559 (1992).

[13] D. G. A. L. Aarts, M. Schmidt, and H. N. W. Lekkerkerker, Science **304**, 847 (2004).

[14] D. G. A. L. Aarts and H. N. W. Lekkerkerker, J. Phys. Condens. Matter **16**, S4231 (2004).

[15] W. K. Wijting, N. A. M. Besseling, and M. A. Cohen Stuart, Phys. Rev. Lett. **90**, 196101 (2003).

[16] S. G. J. M. Kluijtmans and A. P. Philipse, Langmuir **15**, 1896 (1999).

[17] E. Paschinger and G. Kahl, Phys. Rev. E **61**, 5330 (2000).

[18] E. Paschinger, D. Levesque, G. Kahl, and J. J. Weis, Europhys. Lett. **55**, 178 (2001).

[19] M. Schmidt et al., Phys. Rev. Lett. **85**, 1934 (2000).

[20] M. Schmidt, Phys. Rev. E **66**, 041108 (2002); M. Schmidt, E. Schöll-Paschinger, J. Köfinger, and G. Kahl, J. Phys. Condens. Matter **14**, 12099 (2002).

[21] J. M. Brader, R. Evans, M. Schmidt, and H. Löwen, J. Phys. Condens. Matter **14**, L1 (2002).

[22] M. Dijkstra and R. van Roij, Phys. Rev. Lett. **89**, 208303 (2002).

[23] M. L. Rosinberg, E. Kierlik, and G. Tarjus, Europhys. Lett. **62**, 377 (2003).

[24] P. P. F. Wessels et al., J. Phys. Condens. Matter **16**, L1 (2004); **16**, S4169 (2004).

[25] There appears to be a maximum in $\theta$ near $\sigma_m/\sigma_c = 0.8$.

[26] P. P. F. Wessels et al., Phys. Rev. E **68**, 061404 (2003).